



Synergistic Interaction of Coal and Oil-based Wastes During their Co-Pyrolysis

Yelaman Aibuldinov,^{1,2} Nurken Nurgaliyev,^{1,2,*} Eldar Kopishev,³ Zhanar Iskakova,¹ Ainagul Kolpek,³ Ayat Sabitov,^{3,*} Ruslan Muratov,⁴ Galiya Alzhanova,¹ Gaziz Abdiyussupov¹ and Madi Omirzak¹

Abstract

The co-pyrolysis of low-rank coal (LRC) and oil sludge (OS) was investigated at 500 °C under nitrogen with varying mass ratios. The addition of OS (20–80%) enhanced tar and gas yields while reducing char formation, with the most pronounced synergistic effect observed at the 20/80 LRC/OS ratio. Thermogravimetric analysis confirmed improved degradation behavior, showing higher mass loss and lower peak decomposition temperatures compared to theoretical values. At the optimal ratio, the tar composition exhibited increased aromatic hydrocarbons with reduced alkanes and phenols, while gas analysis revealed higher yields of H₂, CH₄, and C_nH_m and lower contents of CO and CO₂. These results demonstrate that co-pyrolysis of LRC and OS is an effective route to valorize hydrocarbon wastes and produce cleaner, energy-rich products.

Keywords: Co-pyrolysis; Low-rank coal (LRC); Oil sludge (OS); Synergistic effect; Pyrolysis tar; TG-DTG-DSC analysis; Hydrogen-rich gases; Waste valorization.

Received: 26 September 2025; Revised: 16 October 2025; Accepted: 20 October 2025

Article type: Research article.

1. Introduction

As high-quality coal reserves decline, the utilization of low-rank coal (LRC) and the management of oil-derived wastes are becoming increasingly important both economically and environmentally.^[1] LRC is abundant and inexpensive, yet its high inherent moisture, low calorific value, and oxygen-rich structure complicate clean conversion and can lead to secondary emissions if not properly handled. In parallel, oil sludge (OS) accumulates across the hydrocarbon value chain and poses persistent environmental risks while retaining significant energy potential.^[2]

Common technologies for LRC utilization include combustion, disposal, gasification, and pyrolysis.^[3] Among them, pyrolysis is considered a cleaner and more energy-efficient approach that enhances feedstock utilization and yields value-added products.^[1] Nevertheless, coal pyrolysis

alone is often economically unfeasible due to the low H/C ratio in coal, resulting in low yields of tar and gas and poor quality of pyrolysis tar.^[4] Additionally, practical utilization of LRC is hampered by the high oxygen content and heavy components in the tar, which complicate downstream processing.^[5] One promising approach to addressing these challenges is co-pyrolysis, which is considered a sustainable strategy for improving product quality and yield.^[6] This is particularly effective when LRC is co-pyrolyzed with hydrogen-rich waste, as it not only enhances tar quality but also facilitates waste valorization.^[5] Such wastes include biomass, plastics, and coal liquefaction residues, which are low-cost, resource-rich, highly volatile, and possess high H/C ratios.^[4]

In the co-pyrolysis of LRC with biomass waste such as rice stalks at varying temperatures (773–1073 K), a high proportion of rice stalk (80%) was shown to reduce the char yield, as the co-pyrolysis suppressed the formation of large aromatic ring structures.^[7] A synergistic effect was also observed in the pyrolysis gas characteristics. In similar experiments with rice straw, a 40 wt.% blend provided the best results, and the strongest synergistic effect was observed within the temperature range of 552–610 K.^[8] A synergistic effect was also found in co-pyrolysis of LRC with straw, though it diminished with increasing straw content.^[9] In a study on microwave-assisted co-pyrolysis of LRC and

¹Research Institute of New Chemical Technologies, L.N. Gumilyov Eurasian National University, Astana, 010008, Republic of Kazakhstan

²Department of Chemistry, Chemical Technology and Ecology, Kazakh University of Technology and Business, Astana, 010000, Republic of Kazakhstan

³Department of Chemistry, Faculty of Natural Sciences, L.N. Gumilyov Eurasian National University, Astana, 010008, Republic of Kazakhstan

macroalgae using 2 wt.% HZSM-5 catalyst, optimal conditions for maximum bio-oil yield (61.7 wt.%) were achieved at a coal/macroalgae ratio of 1:1, with a process time of 135 minutes and power of 450 W.^[10] In a similar study, co-pyrolysis of LRC and microalgae using a bimetallic Cu-Cr-ZSM-5 catalyst produced bio-oil with a higher heating value of 36.5–40.1%, comparable to that of diesel fuel.^[11]

Among hydrogen-rich partners, oil sludge (OS) is particularly attractive: it features a higher H/C, high volatile content, and valuable hydrocarbon fractions (saturates, aromatics, resins, asphaltenes) that can be upgraded into fuels and chemicals; its safe valorization simultaneously addresses an urgent waste-management challenge.^[7] Literature on LRC co-pyrolysis shows composition-dependent synergism in both yields and product distributions, yet systematic evidence for LRC+OS under bench-scale fixed-bed conditions with concurrent yield–quality mapping remains limited.^[12]

Co-pyrolysis of low-rank pulverized coal with direct coal liquefaction residue (DCLR) showed a significant synergistic effect. Both feedstocks acted as hydrogen donors, enhancing hydrogenation of small molecular free radicals, which led to a 5.55% increase in tar yield. The tar composition showed a reduction in aromatic compounds (by 11.88%) and phenols (by 7.94%), while alkanes increased by 12.25%.^[12]

Co-pyrolysis of LRC and polyethylene also led to an increased yield and improved quality of tar, particularly promoting the formation of alkene compounds.^[5] A synergistic effect was also observed in co-pyrolysis of low-rank bituminous coal with polyurethane foam waste.^[13] as well as lignin with LRC.^[14]

The rapid development of the energy sector has created challenges related to the treatment of various types of sludge.^[6,15] Studies have shown that co-pyrolysis of coal and sludge also exhibits catalytic synergistic effects similar to those seen in mixtures of coal and other wastes. Co-pyrolysis of coal and sludge helps reduce pyrolysis activation energy, improve utilization efficiency, and lower sulfur-containing emissions.^[16,17] In the co-pyrolysis of sewage sludge (SS) and low-rank bituminous coal, SS promoted coal pyrolysis and exhibited a synergistic effect, with the maximum gas yield observed at an SS/LRC ratio of 7:3.^[18] Similar findings were reported in other studies,^[19,20] where synergistic interactions enhanced gas evolution and removal of nitrogen and sulfur. At a LRC/SS blend ratio of 50/50, emissions of H₂S and SO₂ were significantly inhibited.^[21] This ratio also proved optimal for bioenergy production, with lower activation energy than at 25% SS addition.^[17] Another study identified optimal LRC/SS ratios of 3–7, providing acceptable environmental impact and satisfactory energy recovery.^[22] Co-pyrolysis of pulp mill

sludge with coal was also reported to increase the coal's reactivity, while the activation energy of the process was lower than the theoretical estimate.^[23,24]

A significant synergistic effect was observed in co-pyrolysis of LRC and heavy oil (HS), resulting in increased tar and gas production.^[25] The tar composition showed an increase in aromatic hydrocarbons (by 21.60%) and a reduction in alkanes (by 7.89%) and phenols (by 8.10%). Co-pyrolysis of oil sludge (OS) and sub-bituminous coal in equal proportions showed that the bound carbon and volatile yields from coal were higher than those from OS.^[26] This co-pyrolysis also enhanced CO production (by 60.3%) and reduced CO₂ emissions (by 26.0%), which the authors attributed to the observed synergistic effect.

Based on the above, there remains a research gap in the co-pyrolysis of LRC with oil-based wastes. Among these, oil sludge (OS) is of particular interest due to its high H/C ratio, high volatile content, and abundant reserves—features it shares with many of the aforementioned waste types. The high crude oil content and calorific value of OS indicate substantial energy potential.^[27] Moreover, OS contains valuable hydrocarbon fractions such as saturated and aromatic compounds, asphaltenes, and resins, which can be recovered and reused as fuels or chemical feedstocks.^[28] Therefore, OS is a highly promising oil waste resource with considerable potential for valorization. In this context, co-pyrolysis of LRC and OS appears to be a feasible and promising approach for achieving more efficient and sustainable hydrocarbon waste utilization. Accordingly, the objective of this work is to investigate the effect of varying mass ratios of LRC and OS on the co-pyrolysis efficiency, with a focus on identifying synergistic interactions that can improve both the yield and quality of pyrolysis products through the interaction of components from both feedstocks.

2. Materials and methods

2.1 Materials

In the present study, low-rank coal was used as the carbonaceous solid feedstock. The coal was sampled from the "Borly" coal deposit located in the Karaganda region of the Republic of Kazakhstan. The raw material consisted of high-ash, fine-fraction coal waste (particle size < 5 mm). After preliminary grinding in a ball mill, the coal was sieved to obtain a fraction with a particle size below 200 μm and then dried for subsequent experiments. Oil sludge was used as the petroleum-based waste material, sourced from the "Uzen" oil field in the Mangystau region of the Republic of Kazakhstan. For both types of feedstock, averaged composite samples were prepared to ensure the reproducibility and reliability of the experimental results.

The characteristics of LRC and OS are summarized in **Table 1**. According to the data, the coal exhibits a high ash content (47.38%) and a low volatile matter yield (22.31%). In contrast, the oil sludge is characterized by an extremely low mineral content (0.23%) and a significantly higher volatile

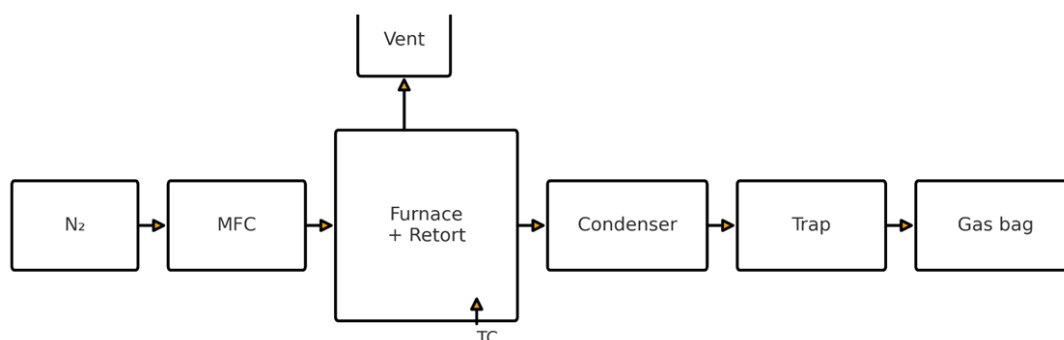
⁴Department of Environmental Management and Engineering, Faculty of Natural Sciences, L.N. Gumilyov Eurasian National University, Astana, 010008, Republic of Kazakhstan

*Email: nurken.nu28@gmail.com (Nurken Nurgaliyev), sabitov_as_1@enu.kz (Ayat Sabitov)

Table 1: Characteristics of the raw materials.

Sample	Proximate analysis (wt%)				Ultimate analysis (wt%)					Molar ratio	
	M	A	V	FC	C	H	O*	N	S	H/C	O/C
LRC	5.34	47.38	22.31	24.97	84.41	5.96	6.94	1.19	1.50	0.84	0.06
OS	24.37	0.23	73.21	2.19	85.20	9.45	2.70	0.39	2.26	1.32	0.02

M: moisture; A: Ash content; V: Volatile matters; FC: Fixed carbon; O*: Oxygen (by difference); N: Nitrogen; S: Sulfur

**Fig. 1:** Simple schematic of the bench-scale fixed-bed co-pyrolysis setup.

matter yield (73.21%). Furthermore, oil sludge contains substantially higher amounts of carbon and hydrogen compared to coal. The hydrogen content in oil sludge is 9.45 wt.%, which positively influences pyrolytic transformations by promoting hydrogen redistribution and enhancing the formation of active hydrogen radicals.^[12] The higher molar H/C ratio of oil sludge compared to coal indicates the predominance of hydrocarbons from the paraffinic and olefinic series. At the same time, the elevated O/C ratio in coal suggests the presence of a larger number of oxygen-containing functional groups, typically associated with compounds such as phenols, aromatic hydrocarbons, aldehydes, and ketones.

For the co-pyrolysis of LRC with OS, a series of samples with varying mass ratios of the two feedstocks were prepared in advance. The compositions ranged from pure coal to pure oil sludge, including intermediate mixtures containing 20% to 80% OS by weight. Accordingly, the mass ratios of LRC/OS were 100/0, 80/20, 60/40, 40/60, 20/80, and 0/100 (wt.%).

2.2 Experimental procedure

The sample materials were air-dried until an approximate equilibrium was reached between the sample moisture content and the ambient atmosphere. The prepared samples were stored in hermetically sealed containers. A 50 g portion of the sample was placed into an aluminum retort and heated under a nitrogen flow of 100 mL/min at a heating rate of 10 °C/min up to a final temperature of 500 °C, with a holding time of 90 minutes. The decomposition products were directed into a receiver cooled with an ice-water mixture.^[12] Tar and water were condensed, while the gaseous products were vented into the atmosphere after sampling for analysis. The overall flow path—nitrogen through the mass flow controller (MFC) into the furnace/retort, followed by condensation, liquid collection,

and gas sampling—is illustrated in Fig. 1.

Nitrogen passes through a mass flow controller into the furnace with a retort (500 °C, 90 min). Volatiles are condensed in an ice-water condenser; liquids are collected in a trap (tar + water); non-condensable gas is sampled in a gas bag for GC analysis. Vent (bubbler/one-way) ensures safe discharge; temperature is monitored by a thermocouple (TC). Following pyrolysis, the yields of liquid products and solid residue were determined gravimetrically, whereas the yield of pyrolysis gas was calculated by mass balance, *i.e.*, as the difference between the initial sample mass and the combined mass of the liquid products and solid residue. All experiments were performed in triplicate, and average values were calculated. Nitrogen flow was controlled by an MFC; temperature at sample height was measured by a K-type thermocouple; liquids were collected gravimetrically and non-condensable gas was sampled in a gas bag for GC.

2.3 Analysis and characterization

To investigate the thermal behavior of the samples during pyrolysis, thermogravimetric analysis (TG-DTA/DSC) was performed using a LABSYS Evo TG-DTA/DSC thermal analyzer (SETARAM, France), which enables simultaneous thermal analysis. This model allows for the concurrent measurement of thermogravimetry (TG), differential thermal analysis (DTA), and differential scanning calorimetry (DSC). Thermal analysis was carried out on 5 mg samples, from room temperature up to 1000 °C, at a heating rate of 20 °C/min. Nitrogen was used as the carrier gas to maintain an inert atmosphere.

Elemental composition of the feedstocks was determined using a Flash EA 1112 automatic elemental analyzer. The composition of the tar was analyzed using a gas

chromatograph–mass spectrometer (GC-MS) GCMS-QP2010 Plus (Shimadzu). Infrared analysis of the pyrolytic char was conducted on a Shimadzu IRTracer-100 FTIR spectrometer equipped with an ATR-8000A module featuring a diamond crystal. The composition of the gaseous products obtained from coal pyrolysis was determined using a Crystallux 4000M gas chromatograph (Meta-Chrom, Russia).

2.4 Calculation theoretical values

To investigate the interactions between LRC and OS during co-pyrolysis, the experimental yields of pyrolysis products (tar, gas, and char), as well as the mass loss of the samples (obtained from TG-DTG-DSC analysis), were compared with the calculated (theoretical) values. The theoretical values were determined under the assumption of no interaction between coal and oil sludge, using weighted average calculations according to Eq. (1)^[29] and (2):^[30]

$$Y_{\text{cal},i} = (1 - x)Y_{\text{LRC},i} + xY_{\text{OS},i} \quad (1)$$

where i denotes the type of pyrolysis product (tar, gas, or char); $Y_{\text{cal},i}$ is the calculated yield of product i from co-pyrolysis; $Y_{\text{LRC},i}$ and $Y_{\text{OS},i}$ are the experimental yields of product i from the pyrolysis of LRC and OS, respectively; and x is the mass fraction of OS in the blend.

The theoretical mass loss (Z_{cal}) of the samples during co-pyrolysis was calculated using Eq. (2):

$$Z_{\text{cal}} = xZ_{\text{LRC}} + yZ_{\text{OS}} \quad (2)$$

where $-$ are the experimental values of mass loss for LRC and OS separately, x and y – are the mass fractions of LRC and OS in the mixture, respectively.

3. Results and discussion

3.1 Yields of pyrolysis products

The results of the co-pyrolysis of LRC and OS are presented in Fig. 2. It was found that the addition of oil sludge in the range of 20% to 80% promotes a more efficient pyrolysis process, as evidenced by a significant increase in tar yield (from 17.06% to 54.31%) and gaseous products (from 9.15% to 28.46%), as well as a sharp reduction in char formation (from 73.79% to 17.23%).

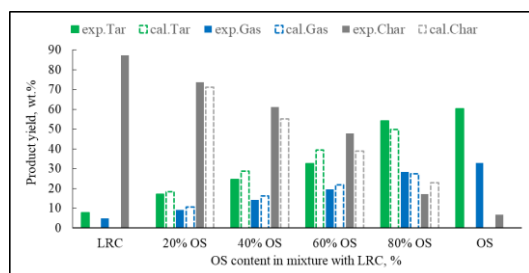


Fig. 2: Effect of varying LRC/OS ratios on the experimental (solid lines) and theoretical (dashed lines) yields of co-pyrolysis products.

This increase in the yield of liquid and gaseous products is likely attributed to the presence in oil sludge of both active hydrogen-donating compounds (e.g., naphthenes and paraffins) and high-molecular-weight components (such as resins and asphaltenes). Hydrogen-donating compounds contribute to the stabilization of free radicals formed during pyrolysis, thereby preventing their recombination into solid products and promoting the formation of liquids and gases. High-molecular-weight compounds, on the other hand, are capable of generating active radicals that initiate the cleavage of strong carbon–carbon and carbon–hydrogen bonds in the coal matrix, thereby enhancing decomposition and increasing the yield of volatile products.

A similar enhancement of product yields was observed during the co-pyrolysis of low-rank coal and heavy oil (at a ratio of 8:2), where tar and gas yields increased by 12.18% and 7.74%, respectively.^[25]

Comparison of the experimental data with the theoretically calculated product yields revealed that a positive synergistic effect occurred only at 80% OS content, at which point the actual yields of tar and gas exceeded the theoretical values. In the remaining samples (with 20% to 60% OS content), the product yields were either comparable to or lower than the theoretical predictions, indicating no positive interaction between the LRC and OS components.

The observed synergistic effect during the co-pyrolysis of LRC with OS is likely due to significant differences in their physicochemical properties. This phenomenon has been previously reported in the scientific literature,^[31] where it was emphasized that substantial differences in the chemical composition and structural characteristics of the feedstocks can promote synergistic interactions during thermal conversion processes. For example, in the co-pyrolysis of biomass and oil sludge, an increase in oil yield and improvement in oil quality were observed, as reflected by an increase in the atomic H/C ratio from 1.5 to 2.0 and an increase in the higher heating value from 19.5 to 24.5 MJ/kg.^[32]

Thus, the results of this study indicate that the optimal LRC/OS ratio is 20/80, which is presumably attributed to several factors. At high oil sludge content, a considerable number of active radicals are generated during the thermal decomposition of OS. These radicals effectively interact with the macromolecular structure of coal, facilitating its breakdown and enhancing the release of volatile compounds. Moreover, the abundance of hydrogen-containing compounds helps stabilize free radicals formed from coal, preventing their recombination and polymerization.

Conversely, at lower oil sludge contents (20–60%), the degree of coal matrix degradation decreases, and the reactions proceed primarily via dehydrogenation and condensation, which limits the formation of liquid and gaseous products. The insufficient amount of hydrogen-donor compounds under these conditions contributes to intensified coking and secondary polymerization of tarry species. Additionally, at high OS content, the oil sludge particles are better distributed

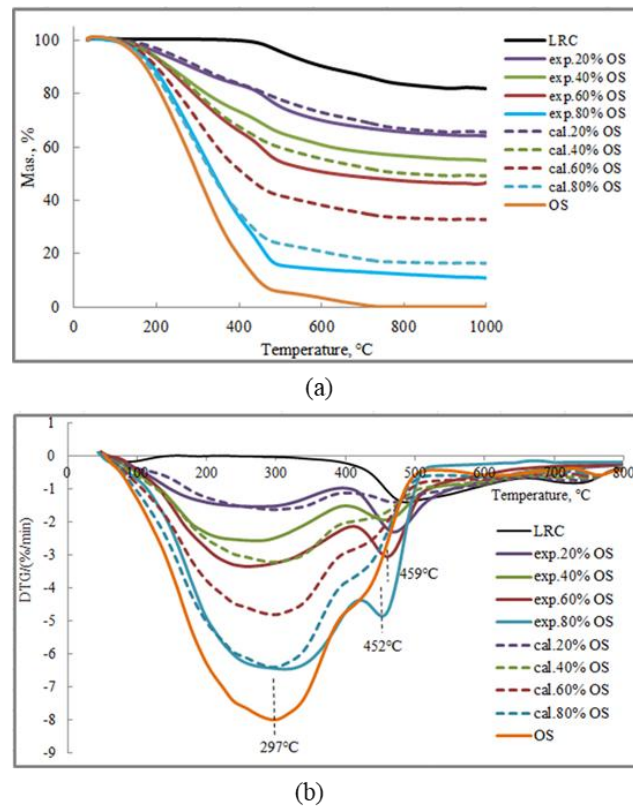


Fig. 3: Experimental and theoretical TG (A) and DTG (B) curves of LRC, OS, and their mixtures.

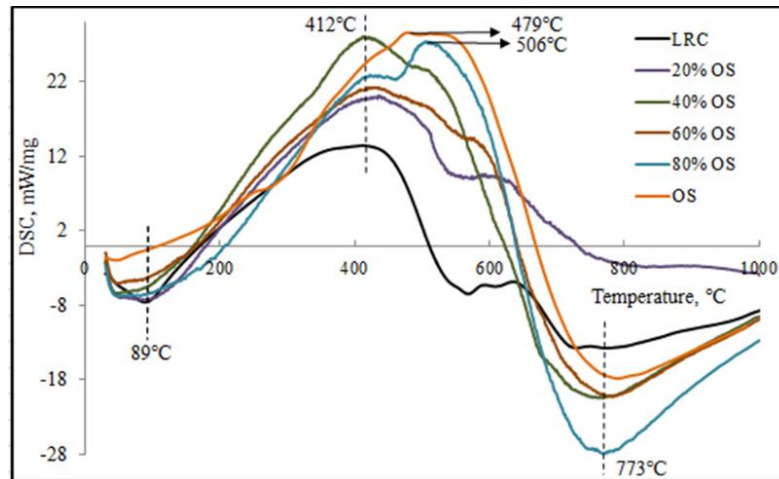


Fig. 4: DSC curves of LRC, OS, and their mixtures.

over the coal surface, which increases porosity and improves heat transfer. This intensifies the liquefaction of the coal structure and significantly enhances tar and gas yields due to more efficient mass and heat transfer processes.

3.2 TG-DTG analysis

Fig. 3 and 4 present the TG-DTG-DSC curves obtained to confirm the synergistic effect between LRC and OS during their co-pyrolysis. The key kinetic parameters corresponding to different LRC/OS mass ratios are summarized in Table 2.

Analysis of the experimental data showed that with an oil sludge content in the range of 20–80%, there is a significant increase in sample mass loss (from 35.9% to 89.03%). The

most pronounced weight loss was observed at 80% OS, exceeding the values recorded for samples with 20–60% OS, as clearly reflected in the TG and DTG curves (Fig. 3), as well as in the maximum weight loss rate (DTG_{max}) and total weight loss values (Table 2). Specifically, at 80% OS, the mass loss increased by 35.79% compared to the 60% OS sample, which represents the highest increment among all tested mixtures.

Moreover, comparison of the experimental and theoretical TG-DTG curves revealed that only the 80% OS sample exhibited experimental curves positioned below the theoretical ones, indicating the presence of a positive synergistic effect. In contrast, the curves for samples with 20–

Table 2: Parameters of pyrolysis characteristics with different additives of oil sludge.

OS content (wt%)	T _{onset}	T _{1max} (°C) / DTG _{1max} (%·min ⁻¹)	T _{2max} (°C) / DTG _{2max} (%·min ⁻¹)	T _{3max} (°C) / DTG _{2max} (%·min ⁻¹)	T _{end}	Weight loss (%)
0	436.03	90.06 / 0.36	506.83 / 1.47	712.84 / 0.55	846.79	16.65
20	132.41	271.33 / 1.54	467.59 / 2.30		839.24	35.90
40	147.32	272.05 / 2.57	455.62 / 1.94		835.69	45.05
60	148.94	257.59 / 3.35	459.05 / 3.05		766.04	53.24
80	151.13	311.07 / 6.46	451.89 / 4.85		818.95	89.03
100	153.52	296.61 / 8.25			703.25	99.07

T_{onset} – onset temperature of pyrolysis; T_{imax} – temperature at which the maximum weight loss rate is reached within a given temperature range; T_{end} – final temperature of pyrolysis.

60% OS were either above or nearly coincident with the theoretical lines, suggesting the absence of synergy or a negative interaction between LRC and OS.

Analysis of the DTG curve for LRC revealed three distinct decomposition stages, with maximum weight loss peaks observed at approximately 90 °C, 507 °C, and 713 °C. These findings are consistent with previously reported data for coals from other deposits.^[12,25,33,34] The small peak at 90 °C corresponds to a low degradation rate and is associated with the drying stage, during which free and inherent moisture is removed.^[3] With the addition of 20% OS, this peak disappears, and a new distinct maximum appears at 271 °C, which shifts toward higher temperatures (around 300 °C) as the OS content increases to 100%. This first decomposition stage for the coal–oil sludge mixtures is the most intense (compared to the second stage) and is primarily associated with the evaporation of low-boiling OS components and the breakdown of weak chemical bonds, resulting in the release of light volatiles and CO₂.^[25]

Upon further heating, the second decomposition stage occurs (peaks around 507–452 °C), which is characterized by a shift in peak temperatures toward lower values. At 100% OS, this peak is no longer observed. This behavior can be attributed to the accelerated decomposition and release of most volatile compounds at this stage. It is likely associated with the breakdown of more stable chemical bonds in the organic matrices of LRC and OS, particularly oxygen-containing functional groups, accompanied by the intensive generation of gaseous products. This stage involves depolymerization, thermal degradation, and recombination of radical fragments with hydrogen atoms, leading to the formation of semi-coke and tarry compounds.^[33] At higher temperatures (third stage), only the LRC sample exhibited a small peak around 713 °C.

Differential scanning calorimetry (DSC) of the LRC sample registered an endothermic peak at 89 °C, corresponding to the drying stage and aligning with the DTG curve. All DSC curves exhibited an exothermic peak in the range of 412–506 °C and an endothermic peak in the range of

757–783 °C across the different LRC/OS ratios. The first peak was significantly more intense than the second, as it corresponds to multiple processes, including organic matrix degradation, dehydrogenation, and semi-coking. The second peak reflects the removal of residual volatiles and coke formation.

The addition of OS led to a shift of the exothermic peak to higher temperatures and a marked increase in its intensity, which is attributed to the high content of volatile components in OS and their intensive thermal decomposition. This effect was particularly pronounced in the DSC curve at 80% OS, which closely resembled that of the 100% OS sample. This observation further confirms the strong positive synergistic effect in co-pyrolysis at this composition.

3.3 Results of the component analysis of pyrolysis tar

The component composition of the liquid products obtained from the pyrolysis of LRC, OS, and their mixture (at a 20/80 ratio) is presented in Table 3. The results showed that the major constituents (over 80%) of the liquid products are aromatic hydrocarbons, alkanes, phenols, and olefins, while alcohols, ketones, and aldehydes are present in smaller amounts.

The higher content of aromatic hydrocarbons and phenols in the pyrolysis tar derived from LRC (compared to OS) may be attributed to its aromatic structure (with a high degree of aromatic ring condensation) and a relatively high amount of oxygen-containing functional groups (–OH, –COOH, –C=O, phenolic groups). The primary pyrolysis reactions of coal are likely to include dehydration, decarboxylation, and aromatization.

In contrast, the liquid product from OS is richer in alkanes and olefins compared to LRC, due to the abundance of long-chain aliphatic hydrocarbons, which, during pyrolysis, undergo homolytic cleavage of C–C bonds within long chains, forming radicals that thermally stabilize as olefins (with double bonds). Therefore, the main pyrolysis reaction pathway for OS is likely cracking of aliphatic chains.

The theoretical percentage content of the components in

Table 3: Component composition of pyrolysis resin.

Sample	Components						
	Alkanes	Olefins	Aromatic Hydrocarbons	Phenols	Alcohols	Ketones	Aldehydes
LRC	12.45	3.18	50.27	15.37	1.51	1.74	1.64
OS	26.45	6.37	34.91	13.24	3.59	0.92	2.07
LRC+OS (20/80)	17.08	3.16	52.27	10.35	2.79	1.30	1.72
Theoretical value	23.65	4.93	37.98	14.47	3.17	1.08	1.98

the liquid product obtained from the co-pyrolysis of coal and oil sludge was calculated using the following Eq. (3):

$$W_{cal} = 0.2W_{LRC} + 0.8W_{OS} \quad (3)$$

where W_{LRC} (%) and W_{OS} (%) –are the percentage contents of the components in the liquid products obtained from the pyrolysis of LRC and OS, respectively.

Analysis of the experimental and theoretical data revealed a significant increase in the concentration of aromatic hydrocarbons in the liquid product from co-pyrolysis, accompanied by a decrease in the proportion of alkanes and phenols. The content of other hydrocarbons changed only slightly. The increased yield of aromatic compounds can be attributed to sequential transformations involving thermal dehydrogenation and cyclization of saturated aliphatic compounds. During pyrolysis, long-chain alkanes and alkyl-aromatic components from OS may undergo dehydrogenation, followed by conversion into cycloalkenes, and subsequently into aromatic structures through ring formation—for example, the generation of polycyclic aromatic hydrocarbons (such as naphthalene) via condensation of simple aromatic molecules (e.g., benzene), with the simultaneous release of hydrogen.

The reduction in alkane content, in turn, may be explained by their thermal instability during pyrolysis, as they tend to undergo homolytic cleavage, forming methane and short-lived radicals. Additionally, the presence of coal contributes radical structures that facilitate hydrogen redistribution and accelerate secondary decomposition of saturated fragments, further decreasing the residual alkane content in the product. One reason for the decreased phenol content may be their hydrogenation by hydrogen radicals, particularly the conversion of phenol to benzene. Phenols may also undergo further transformation into cyclitols, which can decompose into light gaseous hydrocarbons and H_2O .^[25] Other oxygenated compounds present in the liquid product—such as alcohols, ketones, and aldehydes—showed only minor changes, likely due to their relatively low reactivity under the conditions of secondary thermal processes.

As shown in Table 4, the tar derived from LRC was rich in light and medium fractions, accounting for approximately 49% and 36%, respectively, while heavy components represented only about 15%. In contrast, the liquid products obtained from OS showed the opposite trend: light fractions made up only about 20%, whereas medium and heavy

fractions were substantially higher—approximately 49% and 30%, respectively. These differences had a noticeable impact on the composition of the tar formed during co-pyrolysis. Compared to the theoretical values, the proportion of light fractions in the co-pyrolysis product decreased by nearly 5%, which directly led to an increase in the content of medium and heavy fractions. The reduction in light fractions may be attributed to hydrogenation and subsequent cracking of light hydrocarbons in OS into gaseous compounds and water. Additionally, aromatization of light alkanes and olefins may occur, resulting in the formation of heavier aromatic compounds.

Table 4: Changes in Carbon Atom Distribution in Pyrolysis Tar.

Sample	Number of Carbon Atoms		
	C ₆ -C ₁₀	C ₁₁ -C ₁₉	C ₂₀ +
LRC	49.05	36.01	14.94
OS	20.35	49.51	30.14
LRC+OS (20/80)	21.07	50.85	28.08
Theoretical value	26.09	46.81	27.10

3.4 FTIR Analysis results for the char

In the FT-IR spectra, as shown in Fig. 5, six distinct absorption peaks were observed in the following ranges: 3667–3690 cm^{-1} , 2910–2914 cm^{-1} , 1564–1585 cm^{-1} , 1466–1485 cm^{-1} , 1011–1032 cm^{-1} , and 735–785 cm^{-1} .

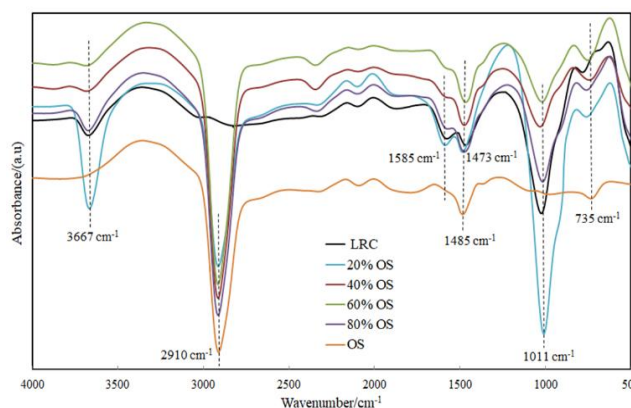


Fig. 5: FTIR spectra of the char.

Table 5: Component Composition of Pyrolysis Gas.

Sample	Components				
	CO, %	H ₂ , %	CH ₄ , %	CO ₂ , %	C _n H _m , %
LRC	27.64	23.41	10.34	20.31	1.53
OS	17.94	35.46	19.67	11.58	3.72
LRC+OS (20/80)	16.03	37.89	20.32	10.41	5.96
Theoretical value	19.88	33.05	17.80	13.33	3.28

The shift in peak positions with increasing OS content may be attributed to transformations in the organic structure involving various functional groups that exert inductive and hydrogen-bonding effects.^[12] The absorption band in the range of 3667–3690 cm⁻¹, corresponding to the stretching vibrations of hydroxyl groups (–OH), indicates the presence of compounds such as alcohols, phenols, and carboxylic acids. However, when the OS content reaches 40%, the intensity of this peak significantly decreases, and these functional groups are no longer detectable at 100% OS.

One of the most intense peaks, observed at 2910–2914 cm⁻¹, is attributed to asymmetric stretching vibrations of methylene groups (–CH₂–), mainly found in aliphatic hydrocarbons. Low-intensity peaks at 1564–1585 cm⁻¹ and 1466–1485 cm⁻¹ correspond to the stretching vibrations of carbonyl groups (C=O) and the bending vibrations of methylene groups (–CH₂–), respectively. Another prominent peak in the range of 1011–1032 cm⁻¹ is associated with out-of-plane vibrations of C–O bonds, suggesting the presence of epoxides and esters on the char surface.

However, similar to the hydroxyl vibration band at 3667–3690 cm⁻¹, the intensity of this C–O peak declines noticeably as the OS content increases beyond 40%. This may be due to the hydrogen released from OS breaking down epoxy structures, thus promoting the formation of gaseous hydrocarbons.^[33] In pure OS, no C–O vibrations are detected, likely because oxygen-containing groups are already destroyed during pyrolysis.

This phenomenon may be attributed to several factors: (1) thermal removal of oxygen in the form of H₂O, CO, and CO₂ via dehydration, decarboxylation, and decarbonylation reactions; (2) cleavage of C–O bonds by hydrogen and hydrocarbon radicals released from OS; and (3) the presence of heavy components in OS (e.g., asphaltenes and resins), which thermally convert into oxygen-poor, stable structures that hinder the formation of new oxygenated compounds.

Finally, the sixth low-intensity peak in the range of 735–785 cm⁻¹ corresponds to bending vibrations of C–H bonds, which are typically found in aromatic rings or alkenes.

3.5 Results of the component analysis of pyrolysis gas

A comparative analysis of the component composition of pyrolysis gas (Table 5) showed that transitioning from the

individual pyrolysis of LRC to that of OS leads to a significant redistribution of gaseous components. In particular, the pyrolysis gas derived from OS exhibits a higher content of hydrogen-containing compounds compared to that from LRC, indicating a greater potential of OS to generate reducing and combustible species during thermal decomposition.

During co-pyrolysis, an increase in the concentrations of H₂, CH₄, and C_nH_m was also observed compared to the theoretical values. This enhancement may be attributed to dehydrogenation reactions, radical chain mechanisms, secondary cracking, and incomplete decomposition of heavy hydrocarbons present in oil sludge. Furthermore, the reduction in CO and CO₂ content may be explained by the occurrence of reduction reactions, such as the conversion of CO₂ to CO or CH₄, and methanation of CO in the presence of excess hydrogen. These secondary processes contribute to the increased formation of combustible gases through the redistribution of oxygen-containing species.

4. Conclusion

The results of this study demonstrated that in the co-pyrolysis of LRC and OS, the oil sludge exerts a significantly greater influence on the efficiency of degradation than coal. Based on the obtained data, the following conclusions can be drawn:

When the LRC/OS ratio was varied from 80/20 to 20/80, tar and gas yields increased substantially—by 37.25% and 19.31%, respectively. This enhancement can be attributed to the high content of active hydrogen-donor compounds and high-molecular-weight components (such as resins and asphaltenes) in OS, which promote the degradation of the coal matrix. Moreover, a positive synergistic effect was observed at the optimal OS content of 80%.

Increasing the OS content in the coal–oil sludge mixture from 20% to 80% led to a 53.13% increase in total mass loss. Thermogravimetric analysis (TG-DTG-DSC) revealed that pyrolysis of coal proceeds through three main decomposition stages. However, upon the addition of 20% OS, the first decomposition peak became broadened, and a new peak emerged around 270 °C. The intensity of this peak (as indicated by DTG_{max}) increased with higher OS content (first stage of co-pyrolysis). The second peak began at approximately 470 °C but shifted downward to around 450 °C with further OS addition. The third peak was only observed

for pure LRC, indicating the catalytic effect of OS on coal decomposition.

The thermal analysis results further confirmed the presence of a synergistic effect at the optimal LRC/OS ratio of 20/80, consistent with the observations made in the fixed-bed retort experiments. At this ratio, the experimental TG and DTG curves were located below the theoretical curves, confirming enhanced degradation behavior.

The analysis of the tar obtained from co-pyrolysis at the optimal LRC/OS ratio revealed a notable increase in the concentration of aromatic compounds compared to theoretical values. Meanwhile, the contents of alkanes and phenols decreased, and the levels of other hydrocarbons remained nearly unchanged. Additionally, the co-pyrolysis process resulted in increased yields of H₂, CH₄, and C_nH_m gases, while the concentrations of CO and CO₂ were reduced.

In summary, the findings of this study highlight the potential of LRC and OS co-pyrolysis as an effective approach for producing value-added products. This method addresses key challenges in the energy sector, particularly those related to the diversification of hydrocarbon feedstocks. Co-pyrolysis of coal and oil sludge represents a promising direction for the development of environmentally friendly and resource-efficient technologies for hydrocarbon waste utilization.

Acknowledgments

This work was carried out with financial support from the Science Committee of the Ministry of Science and Higher Education of the Republic of Kazakhstan (No. BR21882171 "SDG 9.4: Development of the "green" economy of Kazakhstan through the processing of mineral raw materials and waste by pyrolysis").

Conflict of Interest

The authors declare that they have no known competing financial interests or personal relationships that could have appeared to influence the work reported in this paper.

Supporting Information

Not applicable.

CRedit statement

Yelaman Aibuldinov and **Nurken Nurgaliyev**: Writing - Original draft, **Zhanar Iskakova**, **Ainagul Kolpek** and **Ayat Sabitov**: Formal analysis, Data curation, **Eldar Kopishev**, **Galiya Alzhanova** and **Gaziz Abdiyussupov**: Writing - Review & editing, **Madi Omirzak** and **Ruslan Muratov**: Supervision, Conceptualization.

References

- [1] Z. Tian, B. Zhang, Q. Wang, Q. Deng, G. Xu, D. Ma, Effects of different heat carriers on pyrolysis products of high-sodium low-rank coal and optimization of pyrolysis process, *Energy*, 2025, **325**, 136095, doi: 10.1016/j.energy.2025.136095.
- [2] Y. Xia, R. Zhang, Y. Cao, Y. Xing, X. Gui, Role of molecular simulation in understanding the mechanism of low-rank coal flotation: a review, *Fuel*, 2020, **262**, 116535, doi: 10.1016/j.fuel.2019.116535.
- [3] H. Song, G. Liu, J. Zhang, J. Wu, Pyrolysis characteristics and kinetics of low rank coals by TG-FTIR method, *Fuel Processing Technology*, 2017, **156**, 454-460, doi: 10.1016/j.fuproc.2016.10.008.
- [4] L. Wu, Y. Guan, C. Li, L. Shi, S. Yang, B. Rajasekhar Reddy, G. Ye, Q. Zhang, R. K. Liew, J. Zhou, R. Vinu, S. S. Lam, Free-radical behaviors of co-pyrolysis of low-rank coal and different solid hydrogen-rich donors: a critical review, *Chemical Engineering Journal*, 2023, **474**, 145900, doi: 10.1016/j.cej.2023.145900.
- [5] T. Zhang, W. Feng, Z. Bai, H. Zheng, H. Dou, Z. Guo, L. Kong, J. Bai, W. Li, Interpretation of interactions between low rank coal and polyethylene during co-pyrolysis from the bond cleavage perspective, *Journal of the Energy Institute*, 2024, **113**, 101529, doi: 10.1016/j.joei.2024.101529.
- [6] L. Han, J. Li, C. Qu, Z. Shao, T. Yu, B. Yang, Recent progress in sludge co-pyrolysis technology, *Sustainability*, 2022, **14**, 7574, doi: 10.3390/su14137574.
- [7] Y. Zhi, D. Xu, S. Sun, M. Ma, H. Liu, L. Yang, J. Zhao, Co-pyrolysis of low-rank coal and rice stalk: a comprehensive study on product distributions, product properties, and synergistic effects, *Journal of Analytical and Applied Pyrolysis*, 2024, **178**, 106434, doi: 10.1016/j.jaap.2024.106434.
- [8] D. Xu, L. Yang, H. Liu, S. Sun, M. Ma, Y. Zhi, Co-pyrolysis characteristics and kinetics of rice straw and low rank coal, *Journal of Analytical and Applied Pyrolysis*, 2024, **183**, 106741, doi: 10.1016/j.jaap.2024.106741.
- [9] Z. Guo, M. Liu, H. He, F. Song, X. Chen, F. Guo, J. Chen, S. Lu, S. Sang, J. Wu, Co-pyrolysis and co-combustion characteristics of low-rank coal and waste biomass: Insights into interactions, kinetics and synergistic effects, *Journal of the Energy Institute*, 2025, **118**, 101918, doi: 10.1016/j.joei.2024.101918.
- [10] M. Mahfud, A. H. Ramadhana, N. A. Novita, F. Kurniawansyah, B. Sardi, M. Mirzan, L. Mahmudin, A. A. Ali, N. Indrawan, Cleaner production of bio-oil from macroalgae and low-rank coal mixture by pyrolysis in a microwave reactor integrated with a distillation column, *Energy*, 2025, **314**, 134309, doi: 10.1016/j.energy.2024.134309.
- [11] S. Rawat, A. K. Singh, J. P. Chakraborty, S. Kumar, Characterization and mechanism elucidation of high-quality bio-oil production from co-pyrolysis of waste low-rank coal fines and de-oiled microalgae biomass using bimetallic (Cu-Cr) ZSM-5 catalyst, *Journal of Environmental Chemical Engineering*, 2024, **12**, 113046, doi: 10.1016/j.jece.2024.113046.
- [12] Y. Song, N. Yin, D. Yao, Q. Ma, J. Zhou, X. Lan, Co-pyrolysis characteristics and synergistic mechanism of low-rank coal and direct liquefaction residue, *Energy Sources, Part A: Recovery, Utilization, and Environmental Effects*, 2019, **41**, 2675-2689, doi: 10.1080/15567036.2019.1568639.
- [13] Z. M. Banyhani, W. U. H. Khan, H. H. Abd El-Gawad, M.

- Anwar, A. H. Khoja, M. Hassan, R. Liaquat, Z. M. El-Bahy, Synergistic transformation: Kinetic and thermodynamic evaluation of co-pyrolysis for low-rank bituminous coal and polyurethane foam waste, *Process Safety and Environmental Protection*, 2024, **184**, 907-921, doi: 10.1016/j.psep.2024.01.041.
- [14] Y. Fan, B. Yang, B. Zhang, Z. Wu, Z. Sun, J. Shang, Synergistic effects from fast co-pyrolysis of lignin with low-rank coal: On-line analysis of products distribution and fractal analysis on co-pyrolysis char, *Journal of the Energy Institute*, 2021, **97**, 152-160, doi: 10.1016/j.joei.2021.04.009.
- [15] A. Ding, R. Zhang, H. H. Ngo, X. He, J. Ma, J. Nan, G. Li, Life cycle assessment of sewage sludge treatment and disposal based on nutrient and energy recovery: a review, *Science of The Total Environment*, 2021, **769**, 144451, doi: 10.1016/j.scitotenv.2020.144451.
- [16] X. Liu, P. Cui, Q. Ling, Z. Zhao, R. Xie, A review on co-pyrolysis of coal and oil shale to produce coke, *Frontiers of Chemical Science and Engineering*, 2020, **14**, 504-512, doi: 10.1007/s11705-019-1850-z.
- [17] H. Merdun, Z. B. Laougé, A. S. Çığgin, Synergistic effects on co-pyrolysis and co-combustion of sludge and coal investigated by thermogravimetric analysis, *Journal of Thermal Analysis and Calorimetry*, 2021, **146**, 2623-2637, doi: 10.1007/s10973-021-10608-6.
- [18] C. Liu, Z. Shen, H. Zhang, G. He, W. Li, H. Liu, Comprehensive study on co-pyrolysis mechanisms of sewage sludge and low rank coal under rapid/slow heating conditions, *Journal of Analytical and Applied Pyrolysis*, 2025, **185**, 106873, doi: 10.1016/j.jaap.2024.106873.
- [19] L. Mu, J. Chen, P. Yao, D. Zhou, L. Zhao, H. Yin, Evaluation of co-pyrolysis petrochemical wastewater sludge with lignite in a thermogravimetric analyzer and a packed-bed reactor: Pyrolysis characteristics, kinetics, and products analysis, *Bioresource Technology*, 2016, **221**, 147-156, doi: 10.1016/j.biortech.2016.09.011.
- [20] C. He, C. Tang, W. Liu, L. Dai, R. Qiu, Co-pyrolysis of sewage sludge and hydrochar with coals: Pyrolytic behaviors and kinetics analysis using TG-FTIR and a discrete distributed activation energy model, *Energy Conversion and Management*, 2020, **203**, 112226, doi: 10.1016/j.enconman.2019.112226.
- [21] B. Zhao, J. Jin, S. Li, D. Liu, R. Zhang, H. Yang, Co-pyrolysis characteristics of sludge mixed with Zhundong coal and sulphur contaminant release regularity, *Journal of Thermal Analysis and Calorimetry*, 2019, **138**, 1623-1632, doi: 10.1007/s10973-019-08300-x.
- [22] J. Zhou, M. Li, X. Han, B. Wang, C. Zhang, Z. Cheng, Z. Shen, P. C. Ogugua, C. Zhou, X. Pan, F. Yang, T. Yuan, Environmental sustainability practice of sewage sludge and low-rank coal co-pyrolysis: a comparative life cycle assessment study, *Science of The Total Environment*, 2024, **928**, 172255, doi: 10.1016/j.scitotenv.2024.172255.
- [23] R. N. Coimbra, S. Paniagua, C. Escapa, L. F. Calvo, M. Otero, Thermogravimetric analysis of the co-pyrolysis of a bituminous coal and pulp mill sludge, *Journal of Thermal Analysis and Calorimetry*, 2015, **122**, 1385-1394, doi: 10.1007/s10973-015-4834-3.
- [24] R. N. Coimbra, S. Paniagua, C. Escapa, L. F. Calvo, M. Otero, Thermal valorization of pulp mill sludge by co-processing with coal, *Waste and Biomass Valorization*, 2016, **7**, 995-1006, doi: 10.1007/s12649-016-9524-2.
- [25] Y.-H. Song, Q.-N. Ma, W.-J. He, Co-pyrolysis properties and product composition of low-rank coal and heavy oil, *Energy & Fuels*, 2017, **31**, 217-223, doi: 10.1021/acs.energyfuels.6b02106.
- [26] Z.-H. Feng, L. Liu, W.-L. Mo, X.-Y. Wei, J.-R. Yuan, X. Fan, W.-C. Guo, J. Guo, J.-M. Niu, Copyrolysis and cocombustion performance of Karamay oily sludge and Zhundong subbituminous coal, *ACS Omega*, 2022, **7**, 43793-43802, doi: 10.1021/acsomega.2c04854.
- [27] B. Sun, J. Huo, H. Liu, D. Che, S. Guo, Elucidation of synergistic effects in straw/sludge co-pyrolysis through gaseous product monitoring and biochar analysis, *Journal of the Energy Institute*, 2023, **106**, 101151, doi: 10.1016/j.joei.2022.11.011.
- [28] P. Francis Prashanth, B. Shravani, R. Vinu, M. Lavanya, V. Ramesh Prabu, Production of diesel range hydrocarbons from crude oil sludge via microwave-assisted pyrolysis and catalytic upgradation, *Process Safety and Environmental Protection*, 2021, **146**, 383-395, doi: 10.1016/j.psep.2020.08.025.
- [29] Y. Li, S. Huang, Q. Wang, H. Li, Q. Zhang, H. Wang, Y. Wu, S. Wu, J. Gao, Hydrogen transfer route and interaction mechanism during co-pyrolysis of Xilinhote lignite and rice husk, *Fuel Processing Technology*, 2019, **192**, 13-20, doi: 10.1016/j.fuproc.2019.04.022.
- [30] W. Feng, M. Zheng, L. Jin, J. Bai, L. Kong, H. Li, Z. Bai, W. Li, Co-pyrolysis behaviors of coal and polyethylene by combining *in situ* Py-TOF-MS and reactive molecular dynamics, *Fuel*, 2023, **331**, 125802, doi: 10.1016/j.fuel.2022.125802.
- [31] B. Lin, Q. Huang, Y. Chi, Co-pyrolysis of oily sludge and rice husk for improving pyrolysis oil quality, *Fuel Processing Technology*, 2018, **177**, 275-282, doi: 10.1016/j.fuproc.2018.05.002.
- [32] Ning Yin, Y. Song, Lei Wu, P. Dong, C. Wang, Jun Zhou, Xinwei Zhang. Analysis of tar and pyrolysis gas from low-rank coal pyrolysis assisted by apple branch, *Journal Renewable Sustainable Energy*, 2023, **15**(4), 043102, doi: 10.1063/5.0156660.
- [33] N. Yin, Y. H. Song, J. Zhou, Y. H. Tian, A. W. Yang, Effects of direct coal liquefaction residue additions on low-rank pulverized coal during co-pyrolysis, *Materials Science Forum*, 2020, **999**, 167-177, doi: 10.4028/www.scientific.net/msf.999.167.
- [34] N. Liu, H. Huang, X. Huang, R. Li, J. Feng, Y. Wu, Co-pyrolysis behavior of coal and biomass: synergistic effect and kinetic analysis, *ACS Omega*, 2024, **9**, 31803-31813, doi: 10.1021/acsomega.4c03053.

Publisher's Note: Engineered Science Publisher remains neutral with regard to jurisdictional claims in published maps and institutional affiliations.

Open Access

This article is licensed under a Creative Commons Attribution-NonCommercial-NoDerivatives 4.0 International, which permits the use, sharing, adaptation, distribution and reproduction in any medium or format, as long as appropriate credit to the original author(s) and the source is given by providing a link to the Creative Commons license. This usage for commercial purposes is not allowed. If modifications, adaptations or any other transformation were made, it is not allowed for distribution. The images or other third-party material in this article are included in the article's Creative Commons license, unless indicated otherwise in a credit line to the material. If material is not included in the article's Creative Commons license and your intended use is not permitted by statutory regulation or exceeds the permitted use, you will need to obtain permission directly from the copyright holder. To view a copy of this license, visit <https://creativecommons.org/licenses/by-nc-nd/4.0/>.

©The Author(s) 2025.